Characterization and Redesign of Perovskite/Silicon Tandem Cells

Haejun Chung[1], Rahul Singh[1], Lokendra Kumar[2], Muhammad A. Alam[1] *Fellow, IEEE,* and Peter Bermel[1]
[1]School of Electrical and Computer Engineering, Purdue University, West Lafayette, IN 47906, USA
[2]Department of Physics, Science Faculty University of Allahabad, Allahabad-211 002 INDIA

***Abstract*—Recently, metal-halide perovskites/crystalline silicon tandem cells have demonstrated extraordinarily rapid advances in efficiency, now exceeding 21%. However, the incomplete absorption of the bottom c-Si junction has still not been addressed. In this work, we build and characterize perovskite cells to obtain the losses of each layer. We then feed this data into an efficient simulation framework to analyze optical losses of both single and double junction world-record perovskite/silicon cells. Finally, asymmetric dielectric gratings, which are compatible with the fabrication constraints of perovskite/silicon tandem cells, are calculated to yield an increased Jsc of 19.17 mA/cm^2.**

I. Introduction

PEROVSKITE materials represent a uniquely rapid development in PV, where a related set of inexpensive, earth-abundant compounds have risen from very low efficiencies to recently exceed 21% [1]. Nonetheless, their current trend will ultimately approach the Shockley-Queisser limit, about 30% for a bandgap of 1.55 eV. This has given rise to the concept of building perovskite-based tandem cells which can theoretically offer even higher efficiencies [2]–[4]. It seems particularly promising to combine perovskites with crystalline silicon, since both can be manufactured for a relatively low cost and at large scales, while maintaining high efficiencies in tandem. Nonetheless, these cells have a few key limitations so far. First, the bandgap combination of methylammonium lead iodide and crystalline silicon is not ideal. Thus, to have the best current matching, this tandem cell requires very precise photon management near the perovskite band-edge. Several optical studies considered this question already, but there is no clear agreement on the correct top perovskite layer thickness [5]–[7]. The other approach to solve this problem is using a wider-bandgap perovskite materials [8]–[11]. For example, substituting bromine for iodine can extend the perovskite bandgap from 1.5 eV to 2.3 eV [8], but material stability issues remain a key challenge [12].

Second, low energy photon may not be absorbed completely due to the indirect bandgap of bottom silicon cell. In single junction crystalline silicon solar cells, there have been various light trapping studies (e.g., random and periodic conformal texturing) to address this issue [15]. However, in perovskite/silicon tandem cells, the dominant KOH etching technology may not work, due to crucial fabrication constraints [16], [17]. Thus, in this work, we analyze new photon management strategies of experimental perovskite/silicon tandem cells. To do this, we first model the optical dispersion of crucial perovskite materials (e.g., Perovskite, Spiro-OMeTAD, PCBM, PEDOT and TiO_2) in the time domain. These dispersion models are then incorporated into finite difference time domain (FDTD) simulations to analyze both our fabricated single junction perovskite cell and 21% recorded perovskite/silicon tandem cells referred from the literature [16]. This approach allows us to quantify fractional losses in each layer of a tandem cell. Using absorber layer absorption calculated from simulations, we introduce the absorber light harvesting efficiency (ALHE). The ALHE calculated in this study is more useful in some ways than the conventional internal quantum efficiency, because other optical parasitic losses are subtracted by simulation, to help focus on the charge collection efficiency of the absorber only. Thus, the ALHE can characterize purely electrical losses in an absorber, which do not vary much in the same cell fabrication method, even if surrounding layers change. Finally, to address reflection and bulk recombination

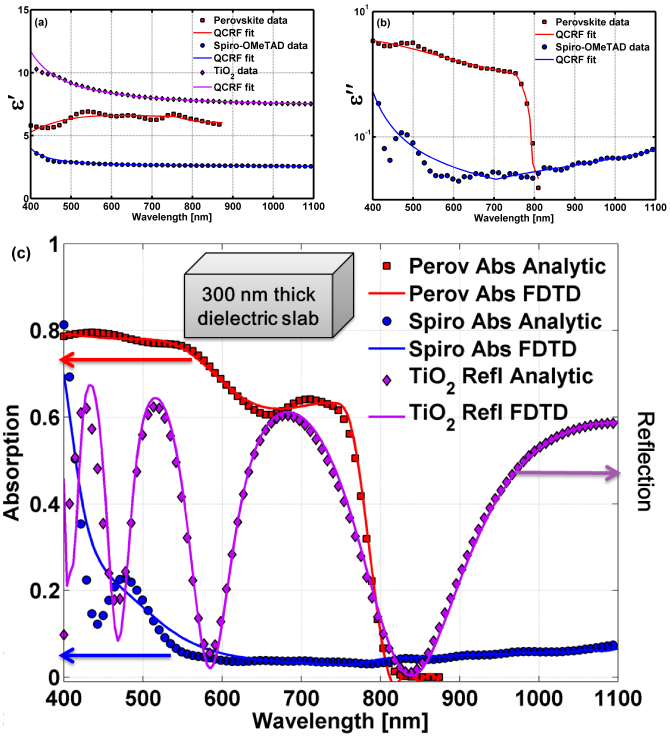

Fig. 1: Dispersion fitting of photovoltaic materials to the QCRF model. The solid lines and symbols indicate the results of the QCRF model and the experimental data [5], [13], [14] of dispersive material, respectively: (a) Real (b) Imaginary part of relative permittivity. (c) The theoretical (symbol) and simulated (line) absorption and reflection spectra of 300-nm-thick material slabs.

losses observed in the experiment, asymmetric dielectric gratings are introduced.

II. Material Modeling

A. Optical modeling

FDTD is a very accurate optical simulation method; however, it requires dispersion functions in the time domain for best performance [18]. We employ Quadratic Complex Rational Function (QCRF) to model perovskite materials [19]. The QCRF method is more accurate and computationally efficient than conventional dispersion models (e.g., Debye and Drude-Lorentz).

As shown in Fig. 1, three representative perovskite solar cell materials are modeled over wavelengths ranging from 400 nm to 1100 nm. The experimental measurement data is collected from Ref [5], [13], [14]. Among the charge collecting layers used in perovskite solar cells, Spiro-OMeTAD is one of the most absorptive. This means it is important to optimize this layer thickness in tandem cell designs [16], [20]. Other dispersive materials (e.g., PCBM, PEDOT:PSS, and silver, etc) are also modeled here, but not shown because of space constraints.

We next apply our QCRF modeling results to the FDTD method. Figure 1.(c) shows a validation of our modeling results in FDTD simulations. For 300-nm-thick dielectric slabs, we calculate transmission and reflection spectra both by FDTD and an analytical equation from our previous work [21]. This result demonstrates that FDTD can predict absorption spectra in perovskite solar cells quite accurately.

B. Single junction perovskite cell fabrication and modeling

Our efficient simulation framework is now applied to analyze fabricated single junction perovskite solar cells. Fabrication of the perovskite cell was performed as follows. First, indium tin oxide (ITO) was cleaned in distilled water, acetone, chloroform, and IPA (10 minutes each). It was then treated with O_2 plasma for 10 min. Poly(3,4-ethylenedioxythiophene) polystyrene sulfonate (PEDOT PSS) was spun coat at 5000 rpm for 45 sec, then dried at 120 C for 20 min. The perovskite solar cell solution was prepared with 0.2 M lead iodide (PbI_2). PbI_2 is mixed with methylammonium chloride (MACl) in a molar ratio of 1:1 in dimethylformamide (DMF) and stirred for 2 days at 70 C before spin-coating on a substrate during the hot-casting process; the substrate is heated to a temperature of 100 C for 2-3 min. During spin coating of the perovskite, it is transferred onto the spin coater chuck. The solution (PbI_2 + MACl) was drop cast onto the substrate, followed immediately by spin coating at 4000 rpm in 15 seconds. Next, the PCBM (20mg/ml) was spun coated at 1000 rpm for 60 sec. Finally, the substrate was transferred to the vacuum chamber for thermal evaporation of a 100 nm-thick Aluminum top contact.

The fractional absorption of each layer of our structure is shown in Fig. 2(a). Unlike perovskite/silicon tandem cells, single junction perovskite cells do not have significant

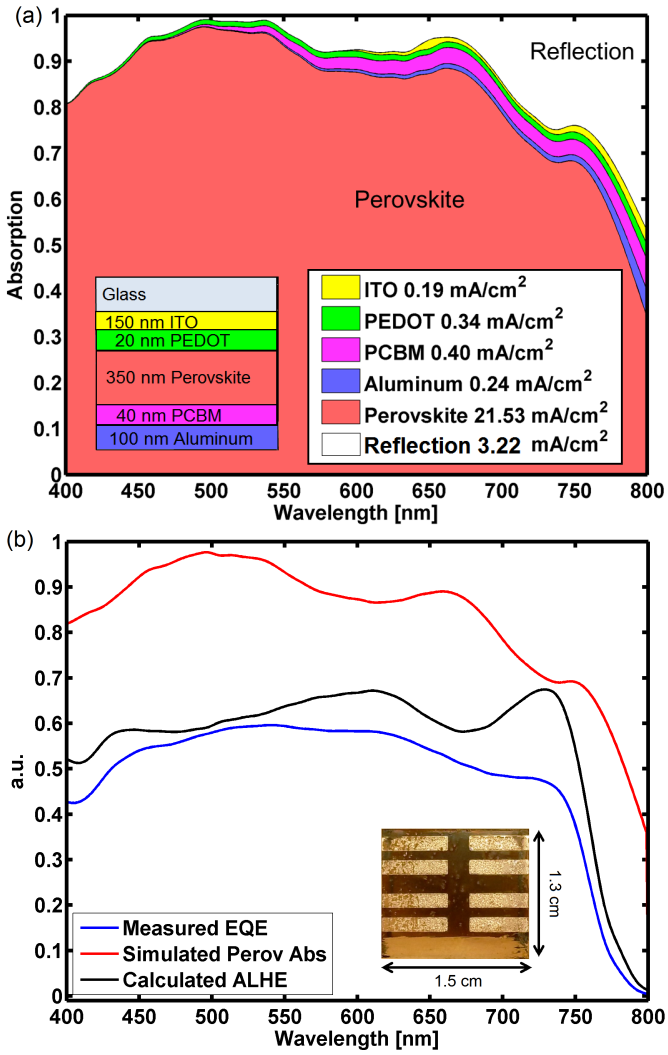

Fig. 2: (a) Optical loss calculation for the fabricated perovskite single junction cell. The inset figure indicates the experimental and simulated cell structure. The combined parasitic loss is 1.17 mA/cm^2 while the reflection loss is 3.22 mA/cm^2 in the simulations. The losses are calculated assuming ideal quantum efficiencies. (b) Absorber light harvesting efficiency (ALHE) is calculated as the experimentally measured EQE divided by the simulated perovskite layer absorption. The inset figure shows our fabricated single junction perovskite cell.

parasitic losses over wavelengths ranging from 400 nm to 800 nm. However, we could expect that substituting our hole collecting layer with Spiro-OMeTAD will slightly increase the parasitic loss in a tandem cell. In this loss analysis, the maximum Jsc is calculated by assuming an ideal internal quantum efficiency (IQE).

Using the fractional absorption of an active perovskite layer, we calculate ALHE $=$ EQE/$A_{perovskite}$, where $A_{perovskite}$ is the simulated fractional absorption of an absorber layer. By analyzing ALHE, pure electrical losses can be separated from parasitic absorption, enabling improved optical structure optimization for a material with given electrical properties. Figure 2 shows the EQE measured and the ALHE calculated in the stabilized perovskite cell. Since

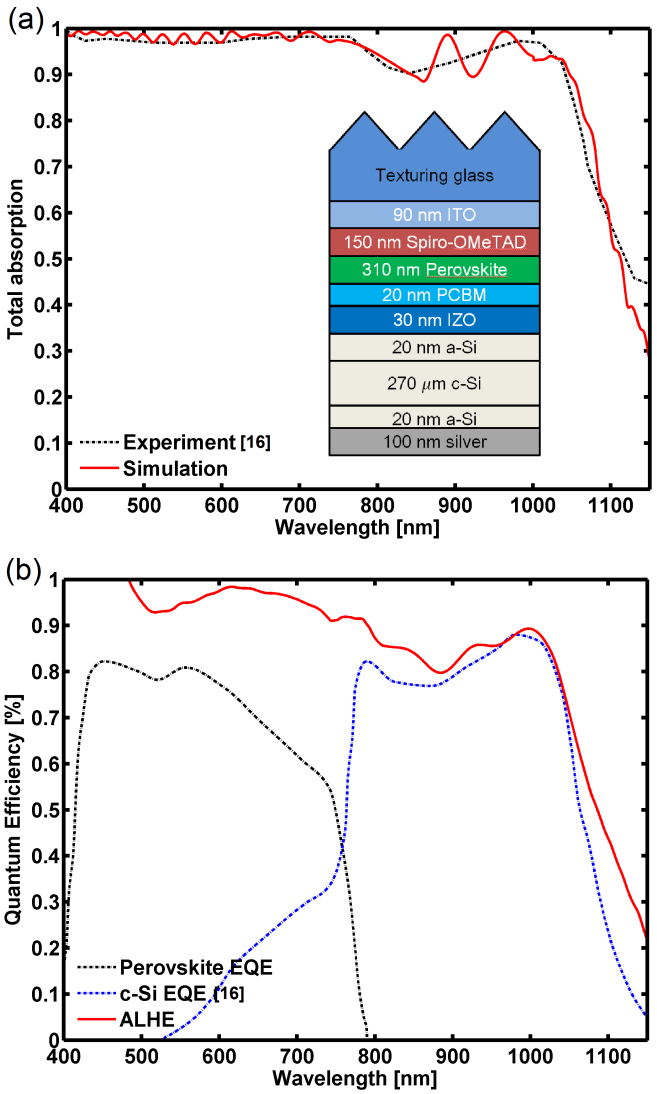

Fig. 3: Perovskite/silicon tandem cell modeling. The experimental absorption and EQE data are collected from [16]. (a) The simulated absorption (using the inset geometry) has a root mean square percent error of 2.26%. (b) The calculated ALHE shows that the perovskite layer does not suffer much electrical losses, while the c-Si layer has recombination losses.

the stabilized EQE measurement gives 13.23 mA/cm^2 while a simulated absorption gives 21.53 mA/cm^2, the difference can be attributed to electrical losses.

C. Tandem perovskite/silicon cell modeling

World-record cell efficiencies of perovskite/silicon tandem cells have risen from 13% [2] to over 21 % [16] within a little over one year. In this work, we analyze the optical losses of these 21% efficiency tandem cells with 3-D FDTD simulations, although the absorption of the wafer-based silicon layer is approximated by a physics-based model [20]. As shown in Fig. 3, the experimental and simulated absorption agree very well, with a root-mean-squared percent error of 2.26 %, which increases our confidence in the following loss calculation. The calculated ALHE shows that the perovskite layer does not suffer much electrical loss, while the c-Si layer has recombination losses at longer wavelengths. This analysis suggests that electrical losses in the crystalline silicon bottom junction need to be improved.

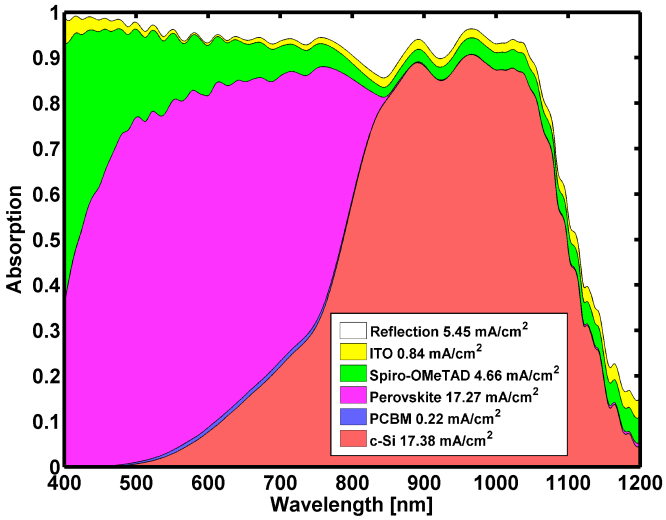

Fig. 4: Optical loss analysis of world-record experimental perovskite/silicon tandem cells [16]. Reflection and Spiro-OMeTAD parasitic absorption are the major loss components over wavelengths ranging from 400–1127 nm. Ideal quantum efficiency is assumed.

As shown in Fig. 4, the two major barriers to ideal optical performance are Spiro-OMeTAD parasitic losses and reflection losses. Unfortunately, adding front texturing to reduce reflection loss, may also increase Spiro-OMeTAD loss due to increased dwell-time, canceling out any potential benefit. Also, a conformal-texturing technology, which can potentially increase light trapping further, may not be compatible with perovskite/silicon tandem cells due to manufacturing constraints [16]. Alternatively, plasmonic back reflector or dielectric back gratings can be used.

III. Light Trapping

In this work, we quantified optical and electrical losses separately for perovskite/silicon tandem cells. Now, we introduce asymmetric dielectric gratings as a potential approach to minimize opto-electrical losses [22]. Dielectric back gratings could be an good alternative light trapping structure for perovskite/silicon tandem cells, because, unlike a conformal texturing, they can be manufactured with a planar silicon top surface.

Pre-optimized asymmetric dielectric gratings are applied to perovskite/silicon tandem cells. They have refractive index of 1.5 and tilting angle of 20 degree. Figure. 5.(a) shows our simulation geometry. It has both front-textured glass and a back dielectric grating, so we decrease c-Si thickness to 10μm, which may be beneficial in reducing bulk recombination loss. As shown in Fig. 5.(b), c-Si Jsc can be increased up to 19.17 mA/cm^2. The reflection loss is also decreased significantly to 0.99 mA/cm^2. Although the experimental perovskite/silicon tandem cells show low

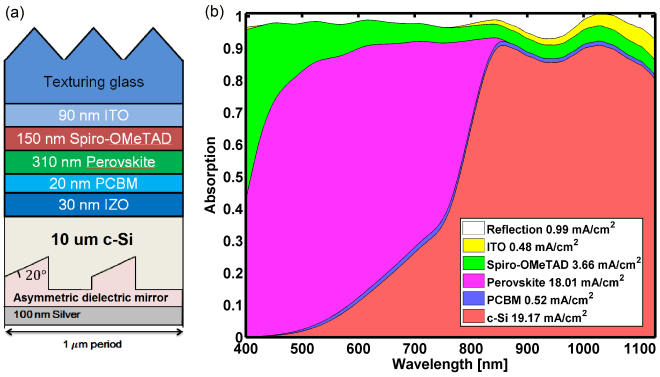

Fig. 5: (a) Light-trapping perovskite/silicon tandem cell simulation geometry (b) Absorption spectrum for the structure in (a).

ALHE at the longer wavelengths, we expect that high quality c-Si cells can convert these low energy photons to electricity.

IV. Conclusion

In conclusion, we quantified both optical and electrical losses separately for perovskite/silicon tandem cells by measuring EQE and simulating the fractional absorption of each layer. The modeled perovskite/silicon tandem cells have 5.45 mA/cm^2 reflection loss and 4.66 mA/cm^2 Spiro-OMeTAD parasitic loss, assuming ideal quantum efficiencies. The experimental tandem cells show nearly perfect absorber light harvester efficiency for a top perovskite junction, while a bottom c-Si junction suffers some recombination losses. Finally, we design a light-trapping structure for perovskite/silicon tandem cells, made of back dielectric gratings, which can be manufactured with a planar silicon top surface. The optimized back grating increases Jsc up to 19.17 mA/cm^2 and reduces reflection loss significantly to 0.99 mA/cm^2 by increasing light trapping at longer wavelengths.

References

[1] M. A. Green, K. Emery, Y. Hishikawa, W. Warta, and E. D. Dunlop, "Solar cell efficiency tables (version 47)," *Progress in Photovoltaics: Research and Applications*, vol. 24, no. 1, pp. 3–11, 2016.

[2] J. P. Mailoa, C. D. Bailie, E. C. Johlin, E. T. Hoke, A. J. Akey, W. H. Nguyen, M. D. McGehee, and T. Buonassisi, "A 2-terminal perovskite/silicon multijunction solar cell enabled by a silicon tunnel junction," *Applied Physics Letters*, vol. 106, no. 12, p. 121105, 2015.

[3] M. R. Khan and M. A. Alam, "Thermodynamic limit of bifacial double-junction tandem solar cells," *Applied Physics Letters*, vol. 107, no. 22, p. 223502, 2015.

[4] R. Asadpour, R. V. Chavali, M. R. Khan, and M. A. Alam, "Bifacial si heterojunction-perovskite organic-inorganic tandem to produce highly efficient (ηt* 33%) solar cell," *Applied Physics Letters*, vol. 106, no. 24, p. 243902, 2015.

[5] M. Filipič, P. Löper, B. Niesen, S. De Wolf, J. Krč, C. Ballif, and M. Topič, "Ch 3 nh 3 pbi 3 perovskite/silicon tandem solar cells: characterization based optical simulations," *Optics express*, vol. 23, no. 7, pp. A263–A278, 2015.

[6] N. N. Lal, T. P. White, and K. R. Catchpole, "Optics and light trapping for tandem solar cells on silicon," *Photovoltaics, IEEE Journal of*, vol. 4, no. 6, pp. 1380–1386, 2014.

[7] B. W. Schneider, N. N. Lal, S. Baker-Finch, and T. P. White, "Pyramidal surface textures for light trapping and antireflection in perovskite-on-silicon tandem solar cells," *Optics express*, vol. 22, no. 106, pp. A1422–A1430, 2014.

[8] D. P. McMeekin, G. Sadoughi, W. Rehman, G. E. Eperon, M. Saliba, M. T. Hörantner, A. Haghighirad, N. Sakai, L. Korte, B. Rech *et al.*, "A mixed-cation lead mixed-halide perovskite absorber for tandem solar cells," *Science*, vol. 351, no. 6269, pp. 151–155, 2016.

[9] Q. Han, S.-H. Bae, P. Sun, Y.-T. Hsieh, Y. M. Yang, Y. S. Rim, H. Zhao, Q. Chen, W. Shi, G. Li *et al.*, "Single crystal formamidinium lead iodide (fapbi3): Insight into the structural, optical, and electrical properties," *Advanced Materials*, 2016.

[10] K. A. Bush, C. D. Bailie, Y. Chen, A. R. Bowring, W. Wang, W. Ma, T. Leijtens, F. Moghadam, and M. D. McGehee, "Thermal and environmental stability of semi-transparent perovskite solar cells for tandems enabled by a solution-processed nanoparticle buffer layer and sputtered ito electrode," *Advanced Materials*, 2016.

[11] R. E. Beal, D. J. Slotcavage, T. Leijtens, A. R. Bowring, R. A. Belisle, W. H. Nguyen, G. F. Burkhard, E. T. Hoke, and M. D. McGehee, "Cesium lead halide perovskites with improved stability for tandem solar cells," *The journal of physical chemistry letters*, vol. 7, no. 5, pp. 746–751, 2016.

[12] C. D. Bailie and M. D. McGehee, "High-efficiency tandem perovskite solar cells," *MRS Bulletin*, vol. 40, no. 08, pp. 681–686, 2015.

[13] Y. Jiang, M. A. Green, R. Sheng, and A. Ho-Baillie, "Room temperature optical properties of organic–inorganic lead halide perovskites," *Solar Energy Materials and Solar Cells*, vol. 137, pp. 253–257, 2015.

[14] A. J. Moulé and K. Meerholz, "Interference method for the determination of the complex refractive index of thin polymer layers," *Applied Physics Letters*, vol. 91, no. 6, p. 061901, 2007.

[15] P. Papet, O. Nichiporuk, A. Kaminski, Y. Rozier, J. Kraiem, J.-F. Lelievre, A. Chaumartin, A. Fave, and M. Lemiti, "Pyramidal texturing of silicon solar cell with tmah chemical anisotropic etching," *Solar Energy Materials and Solar Cells*, vol. 90, no. 15, pp. 2319–2328, 2006.

[16] J. Werner, C.-H. Weng, A. Walter, L. Fesquet, J. P. Seif, S. De Wolf, B. Niesen, and C. Ballif, "Efficient monolithic perovskite/silicon tandem solar cell with cell area¿ 1 cm2," *The journal of physical chemistry letters*, 2016.

[17] S. Albrecht, M. Saliba, J. P. C. Baena, F. Lang, L. Kegelmann, M. Mews, L. Steier, A. Abate, J. Rappich, L. Korte *et al.*, "Monolithic perovskite/silicon-heterojunction tandem solar cells processed at low temperature," *Energy & Environmental Science*, 2015.

[18] A. Tavlove and S. C. Hagness, "Computational electrodynamics: the finite-difference time-domain method," *Artech House, Norwood, MA*, vol. 2062, 1995.

[19] H. Chung, S.-G. Ha, J. Choi, and K.-Y. Jung, "Accurate fdtd modelling for dispersive media using rational function and particle swarm optimisation," *International Journal of Electronics*, vol. 102, no. 7, pp. 1218–1228, 2015.

[20] H. Chung, X. Sun, and P. Bermel, "Optical approaches to improving perovskite/si tandem cells," *MRS Advances*, vol. 1, no. 14, pp. 901–910, 2016.

[21] H. Chung, K. Jung, X. Tee, and P. Bermel, "Time domain simulation of tandem silicon solar cells with optimal textured light trapping enabled by the quadratic complex rational function," *Optics Express*, vol. 22, no. 103, pp. A818–A832, 2014.

[22] H. Chung, C. Zhou, X. Tee, K. Jung, , and P. Bermel, "Hybrid dielectric light trapping designs for thin-film cdznte/si tandem cells," *Optics Express*, vol. 24, no. 14, pp. A1008–A1020, 2016.